Second Window Surveillance: Albumin-Complexed Semiconducting Polymers for NIR-II Fluorescence Imaging of Pan-Ovarian Cancer

Isabella Vasquez (Undergraduate)[1,2,3], Md Shahriar[4], Asma Harun[2,3], Prof. Ulrich Bickel[3,5], Prof. Changxue Xu[4], Prof. Indrajit Srivastava[2,3,*]

[1] Dept. of Chemistry & Biochemistry, Texas Tech University, Lubbock, TX, [2] Dept. of Mechanical Engineering, Texas Tech University, Lubbock, TX, [3] Texas Center for Comparative Cancer Research (TC3R) Amarillo, TX, [4]Dept. of Industrial, Manufacturing, and Systems Engineering, Texas Tech University, Lubbock, TX; [5]Dept. of Pharmaceutical Sciences, Jerry H. Hodge School of Pharmacy, Texas Tech University Health Science Center, Amarillo, TX 79106, United States

*indrajit.srivastava@ttu.edu

TEXAS TECH™

the Srivastava LAB

Introduction

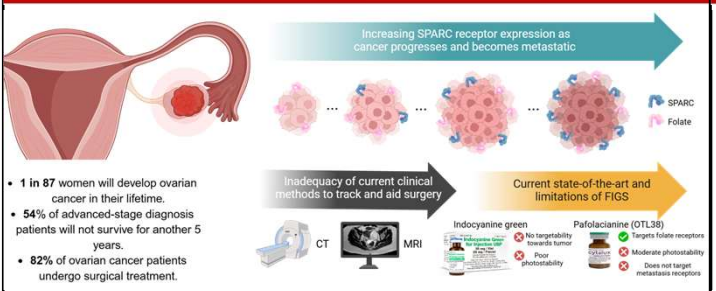

Figure 1. Overview of current ovarian cancer treatment methods with inadequacies addressed by modern FIGS methods. Stats. obtained from American Cancer Society (2023), National Cancer Database (2003-2011) & John, B. et al. Oncogene 2019, 38, 4366.

Our Approach

Figure 2. Schematic overview of albumin nanoparticle (NP) design with increased NIR-II fluorescence, ovarian cancer receptor targeting, and improved stability. These desired features of the NP design are to be evaluated by several 2D and 3D *in vitro* assessments, microfluidic on-chip analysis, and *in vivo* cancer models.

Preliminary Screening of Protein Candidates

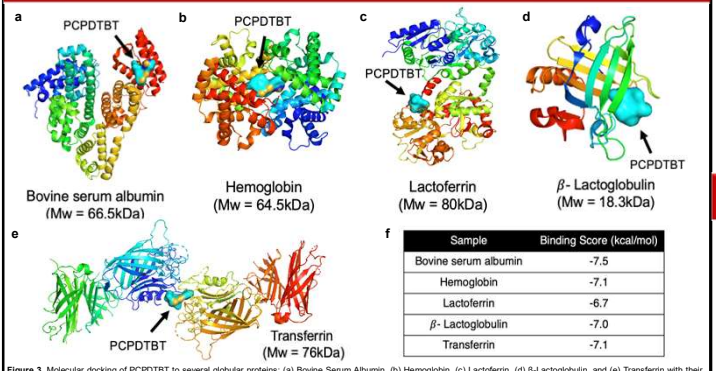

f

Sample	Binding Score (kcal/mol)
Bovine serum albumin	-7.5
Hemoglobin	-7.1
Lactoferrin	-6.7
β- Lactoglobulin	-7.0
Transferrin	-7.1

Figure 3. Molecular docking of PCPDTBT to several globular proteins: (a) Bovine Serum Albumin, (b) Hemoglobin, (c) Lactoferrin, (d) β-Lactoglobulin, and (e) Transferrin with their respective binding scores in (kcal/mol) (f).

Nanoengineering Synthesis Approach

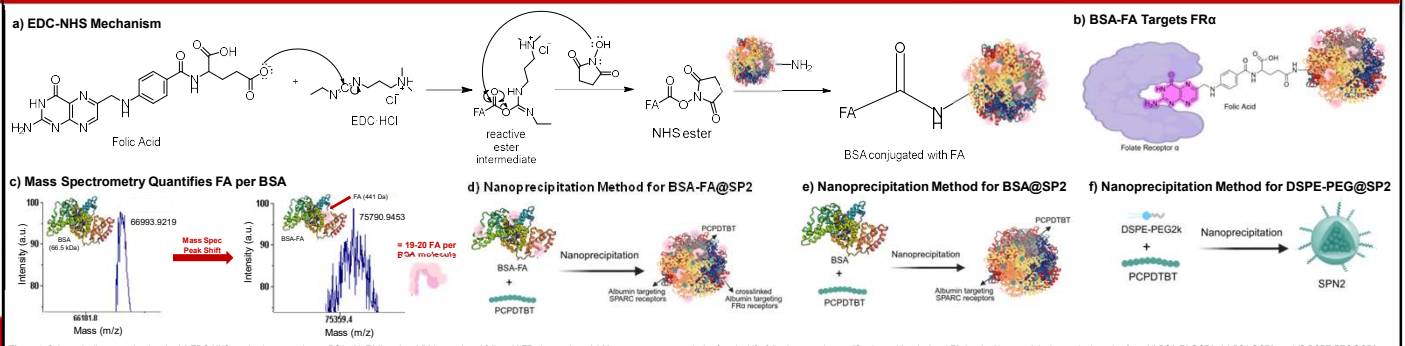

Figure 4. Schematic diagrams showing the (a) EDC-NHS mechanism to conjugate BSA with FA ligand and (b) its employed folic acid-FRα interactions. (c) Mass spectrometry analysis of peak shifts following targeting modifications with calculated FA density. Nanoprecipitation method used to form (d) BSA-FA@SP2, (e) BSA@SP2, and (f) DSPE-PEG@SP2.

BSA Concentration Optimization for Nanoprecipitation

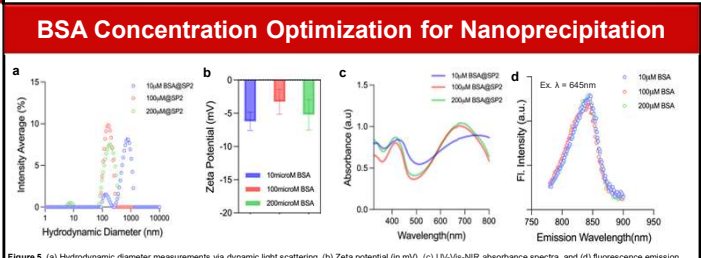

Figure 5. (a) Hydrodynamic diameter measurements via dynamic light scattering, (b) Zeta potential (in mV), (c) UV-Vis-NIR absorbance spectra, and (d) fluorescence emission spectra (λ_{exc} =645 nm) of 10μm, 100μm, and 200μm BSA coated SP2 nanoparticle solutions with fixed SP2 dye concentration.

Physiochemical Characterization

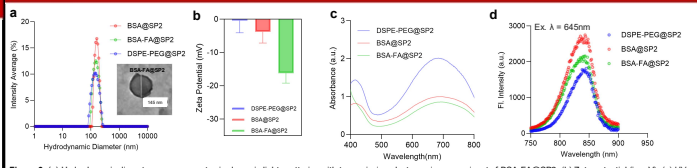

Figure 6. (a) Hydrodynamic diameter measurements via dynamic light scattering with transmission electron microscopy inset of BSA-FA@SP2, (b) Zeta potential (in mV), (c) UV-Vis-NIR absorbance spectra, and (d) fluorescence emission spectra (λ_{exc} =645 nm) of DSPE-PEG@SP2, BSA@SP2, and BSA-FA@SP2.

Improved NIR-II Fluorescence *via* Albumin Chaperoning

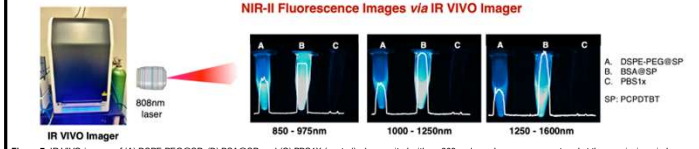

Figure 7. IR VIVO images of (A) DSPE-PEG@SP, (B) BSA@SP, and (C) PBS1X (control) when excited with an 808nm laser. Images were captured at three emission windows: NIR-I (850 – 975 nm), NIR-II (1000 – 1250 nm), and LP125 (1250 – 1600 nm).

On-Chip Platform to Evaluate Tumor Uptake

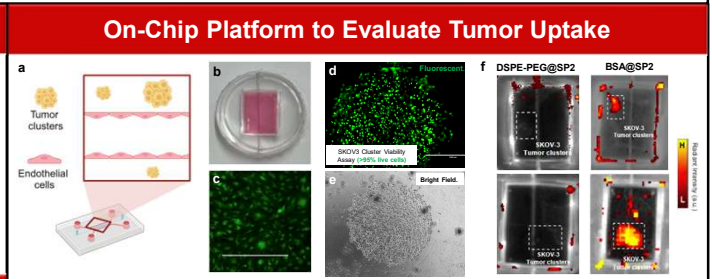

Figure 7. (a) Microfluidic chip design with tumor cluster and endothelial cell layers surrounding focus channel. (b) White light image of microfluidic chip device. (c) Confocal microscope image of HUVECs used for channel lining. (d) Fluorescent viability image and (e) corresponding bright field image of SKOV3 tumors following NP incubation. (f) Fluorescence image of an on-chip model designed with SKOV3 tumor clusters, showing internalization signals of DSPE-PEG@SP2 and BSA@SP2 nanoparticles.

Conclusion and Ongoing Work

1. Bovine Serum Albumin (BSA) exhibits a strong binding affinity towards PCPDTBT due to the availability of drug-binding sites and well-characterized hydrophobic pockets.
2. BSA-chaperoned nanoparticles improve NIR-II fluorescence abilities by red-shifting the emission into a 1250 – 1600 nm range.
3. BSA- chaperoned nanoparticles experience increased cellular uptake by SKOV3 compared to a traditional lipid coating (DSPE-PEG2k), suggesting active cellular internalization pathways via the SPARC receptor.

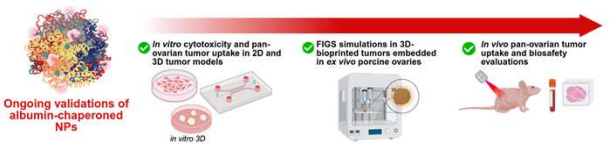

Acknowledgments

We would like to acknowledge the Edward E. Whitacre Jr. College of Engineering at Texas Tech University, the American Heart Association, and The Robert A. Welch Foundation for providing laboratory funding to the Srivastava Lab. The Cancer Prevention & Research Institute of Texas provided support for NIR-II imaging with the IR VIVO imager. We would also like to acknowledge Hasnat Rashid for the TEM image used in this presentation.

American Heart Association. 25IRE1372884

Cancer Prevention & Research Institute of Texas RP200572

Edward E. Whitacre Jr. College of Engineering

The Welch Foundation X-D-015-20250717